Journal of Solid State Chemistry 182 (2009) 2526–2529

Contents lists available at ScienceDirect

Journal of Solid State Chemistry

journal homepage: www.elsevier.com/locate/jssc

Magnetic properties of $Co_2V_2O_7$ single crystals grown by flux method

Zhangzhen He [a,*], Jun-Ichi Yamaura [b], Yutaka Ueda [b], Wendan Cheng [a,*]

[a] State Key Laboratory of Structural Chemistry, Fujian Institute of Research on the Structure of Matter, Chinese Academy of Sciences, Fuzhou, Fujian 350002, People's Republic of China

[b] Institute for Solid State Physics, University of Tokyo, Kashiwa, Chiba 277-8581, Japan

ARTICLE INFO

Article history:
Received 29 April 2009
Received in revised form
7 June 2009
Accepted 6 July 2009
Available online 10 July 2009

Keywords:
Vanadium oxides
Crystal growth
Magnetic property

ABSTRACT

Based on the phase diagram of CoO–V_2O_5 system, single crystals of $Co_2V_2O_7$ are grown using V_2O_5 as self-flux at a slow cooling rate. The quality of grown crystals is analyzed by X-ray powder diffraction and electron probe microanalysis techniques. Magnetic properties are investigated by means of susceptibility, magnetization, and heat capacity measurements. Our experimental results suggest that $Co_2V_2O_7$ is a three-dimensional antiferromagnet, in which two magnetic transitions may occur at low temperature and a spin-flop-like transition may occur at the applied field along the *b*-axis. By contrast to $Ni_2V_2O_7$, it is suggested that similar and different magnetic properties may arise from their similar crystal structures and different magnetic ions, respectively.

1. Introduction

Compounds with a general formula of $M_2X_2O_7$ (M = Cu, Co, Ni, Fe, Mn; X = P, As, V) have been an active field in solid-state chemistry and physics, because of their rich structural features and interesting magnetic behaviors [1–10]. In general, $M_2X_2O_7$ are composed of M^{2+} cations in octahedral coordination and $(X_2O_7)^{4-}$ anions with corner-sharing bitetrahedra, which are found to have two structural categories: thortveitite ($Sc_2Si_2O_7$) and dichromate ($K_2Cr_2O_7$). The significant structural difference between them depends on $(X_2O_7)^{4-}$ anions, in which two tetrahedral XO_4 co-share an oxygen atom in a staggered conformation with a linear X–O–X moiety or an eclipsed one with a bent X–O–X linkage in the thortveitite or dichromate structures, respectively. Due to their interesting structural features, magnetic properties of $M_2X_2O_7$ have also been investigated extensively. Among them, we recently found unusual properties of large paramagnetic anisotropy and spin-flop transition in $Cu_2V_2O_7$ [11] and a martensitic-like transition in $Mn_2V_2O_7$ [12,13].

Two vanadates of this family, $Ni_2V_2O_7$ and $Co_2V_2O_7$, are found to have a similar structure, which crystallize in a monoclinic system of space group $P2_1/c$ [14]. As shown in Fig. 1, both of $(V_2O_7)^{4-}$ anions occur in an eclipsed conformation with V–O–V angle of ~117.5°, indicating that $Ni_2V_2O_7$ and $Co_2V_2O_7$ belong to the dichromate structures. One of the most remarkable structural features is that magnetic Ni^{2+}/Co^{2+} ions have two crystallographic sites with the arrays of edge-shared NiO_6/CoO_6 octahedra forming skew chains along the *c*-axis, and the skew chains are separated by nonmagnetic bitetrahedral $(V_2O_7)^{4-}$, resulting in a quasi-1D structural arrangement.

It is well known that magnetic properties of compounds are closely related to their crystal structure and the compounds with the same crystal structure display likely similar magnetic ground states. In recent study, $Ni_2V_2O_7$ has been found to behave as a typical three-dimensional (3D) antiferromagnet, in which three magnetic orderings occur at low temperature and a metamagnetic-like transition occurs at the applied filed along the *a*-axis [15]. A preliminary magnetic investigation on polycrystalline samples have suggested that $Co_2V_2O_7$ seems to be ferromagnetic [3], which is different from antiferromagnetic $Ni_2V_2O_7$. To understand such differences between $Ni_2V_2O_7$ and $Co_2V_2O_7$, and to further investigate the changes in their magnetic properties of $M_2V_2O_7$ with different magnetic M ions such as Cu^{2+}, Ni^{2+}, Co^{2+}, Fe^{2+} and Mn^{2+}, a single crystal sample is required for magnetic measurements. In this paper, single crystals of $Co_2V_2O_7$ are successfully grown by flux method and the magnetic properties are investigated by means of magnetic and heat capacity measurements.

2. Experimental section

A polycrystalline sample of $Co_2V_2O_7$ was synthesized by a standard solid-state reaction method using a mixture of high purity reagents of $CoC_2O_4 \cdot 2H_2O$ (3N) and V_2O_5 (4N) in the molar ratio of 2:1. The mixture was ground carefully, homogenized thoroughly with ethanol (99%) in an agate mortar, and then packed into an alumina crucible and calcined at 600 °C in air for

* Corresponding authors.
E-mail addresses: hcz1988@hotmail.com (Z. He), cwd@fjrism.ac.cn (W. Cheng).

0022-4596/$ - see front matter © 2009 Elsevier Inc. All rights reserved.
doi:10.1016/j.jssc.2009.07.005

60 h with several intermediate grindings. Crystal growth of $Co_2V_2O_7$ was carried out in a commercial electric furnace. The mixture of polycrystalline $Co_2V_2O_7$ and V_2O_5 with a ratio of 2:1 was melted in an alumina crucible ($\Phi 42 \times 50\,mm^3$) and then the crucible was capped with a cover using Al_2O_3 cement (C-989, Cotronics Corp.). Such closed crucible was put into the furnace and then the furnace was heated up to 900 °C and kept at 900 °C for 10 h to ensure that the solution melts completely and homogeneously. The furnace was slowly cooled to 700 °C at a rate of 1 °C/h and then cooled to room temperature at a rate of 100 °C/h. With this procedure, $Co_2V_2O_7$ crystals with an irregular morphology in Fig. 2 were obtained by mechanical separation from the crucible.

X-ray powder diffraction (XRD) data were collected at room temperature in the range $2\theta = 5$–90° with a scan step width of 0.02° using an MXP21AHF (Mac Science) powder diffractometer with graphite monochromatized Cu$K\alpha$ radiation. The crystal structure was refined by the Rietveld method using the RIETAN-2000 program [16]. Chemical analysis was performed using an electron probe microanalysis (EPMA) system (JEOL JSM-5600 · Oxford Link ISIS). Magnetic susceptibility and magnetization were preformed using a superconducting quantum interference device (MPMS5S, Quantum Design) magnetometer. Heat capacity was measured by a relaxation method using a commercial physical property measurement system (PPMS, Quantum Design).

3. Results and discussion

The phase diagram of CoO–V_2O_5 system has been studied in detail [17], showing three different compositions including CoV_2O_6, $Co_2V_2O_7$, and $Co_3V_2O_8$ in this binary system. It is clear that the grown crystal is not $Co_2V_2O_7$ but $Co_3V_2O_8$ while the melt of stoichiometric composition of $Co_2V_2O_7$ is cooled. This shows that $Co_2V_2O_7$ exhibits an incongruent melting feature. Thus it is necessary to use the flux method for the growth of single crystals. To avoid impurity from flux into the grown crystals, we selected one of starting materials V_2O_5 to be self-flux. After we tested different ratios of V_2O_5, it was found that the molar ratio of $Co_2V_2O_7$:$V_2O_5 = 2:1$, which corresponds to that of CoO:$V_2O_5 = 1:1$, is suitable for the growth of $Co_2V_2O_7$ single crystals and a further increase of V_2O_5 can lead to the appearance of monoclinic CoV_2O_6 phase [18]. As discussed in Ref. [19–21], to grow single crystals of vanadium-based oxides with high quality, many important points of growth process are noted as follows: to allow slow spontaneous nucleation in the melt, the growth must be done at a very slow cooling rate. Furthermore, to avoid the inclusions of the melt into the crystal due to overcool of the melt, the furnace needs to be kept at a constant temperature several times in the cooling process. In addition, to carefully avoid the evaporation of V_2O_5 at high temperature resulting in an unsteady solution system during the growth, the alumina crucible is capped with a cover using Al_2O_3 cement to be a closed system.

The quality of grown crystals was confirmed by XRD and EPMA techniques. A typical XRD pattern was obtained using the crushed crystals. Fig. 3 shows the observed and calculated XRD patterns for $Co_2V_2O_7$. Indexing the Bragg reflections, it is found that all peaks can be indexed with the monoclinic system. No phase impurity can be detected. The observed XRD pattern agrees closely with the simulated one which was obtained as a refinement by the Rietveld method. A full matrix refinement with 48 refined parameters was performed, giving final reliability factors $R_{wp} = 4.65\%$, $R_p = 3.01\%$, and $S = 2.82$. The lattice constants of $a = 6.589(6)$ Å, $b = 8.409(1)$ Å, $c = 9.496(8)$ Å, and $\beta = 100.12(6)^\circ$ obtained from the Rietveld refinement are in good agreement with those reported previously [14]. Since $Co_2V_2O_7$ is an insulator, the surfaces of sample need to be coated with carbon for element analysis using EPMA system. The inset of Fig. 3 shows a typical EDS spectrum of $Co_2V_2O_7$. No other metal elements except for Co and V were confirmed. The molar ratio of Co:V was calculated to be approximately 1:1, which is consistent with the

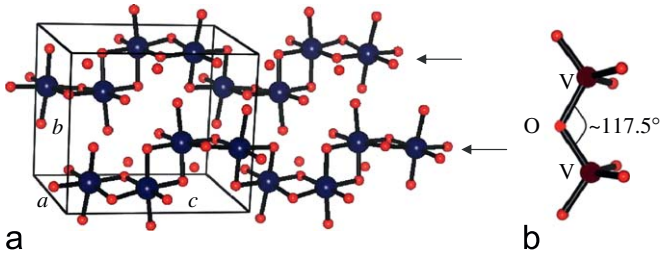

Fig. 1. Crystal structure of $M_2V_2O_7$ (M = Ni and Co): (a) skew-chains built by M ions along the c-axis and (b) $(V_2O_7)^{4-}$ anions with V–O–V angle of ~117.5°.

Fig. 2. Single crystals of $Co_2V_2O_7$ with an irregular morphology.

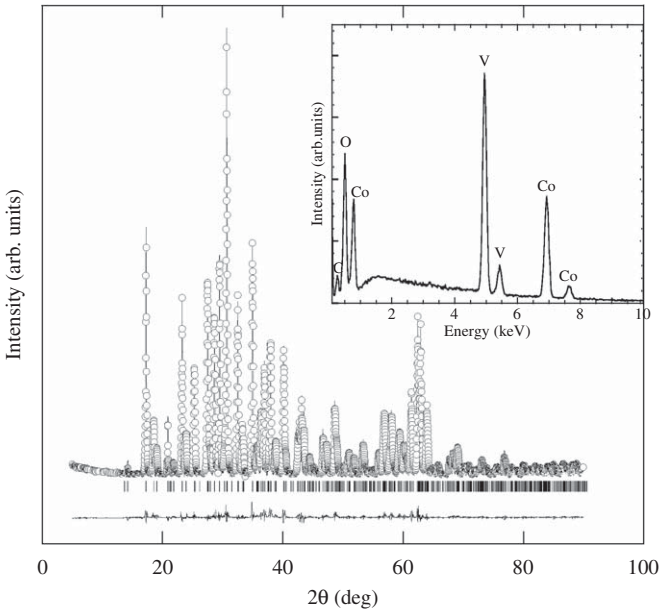

Fig. 3. Observed (open circles) and calculated (solid line) XRD pattern for $Co_2V_2O_7$. The difference is shown at the bottom and Bragg reflections are indicated by vertical marks. The inset shows a typical EDS spectrum acquired from a $Co_2V_2O_7$ crystal coated with carbon.

formula of $Co_2V_2O_7$. These results show that the grown crystals are $Co_2V_2O_7$ and have good quality.

A selected crystal was polished to be plate-like for magnetic measurements. The orientations of the surfaces were determined using a Bruker SMART three-circle diffractometer equipped with a CCD area detector. Fig. 4 shows magnetic susceptibility and corresponding reciprocal one measured in an applied field of 0.1 T along *c*-axis. The susceptibility increases with decreasing temperature, while a sharp peak is observed around ~6 K, showing the onset of antiferromagnetic (AF) ordering. The susceptibility above 110 K follows well the Curie–Weiss law, giving the Curie constant $C = 7.00(6)$ emu K/mol and Weiss constant $\theta = -13.3(3)$ K. The effective magnetic moment (μ_{eff}) is calculated to be $5.29(3)\,\mu_B$, which is quite larger than the value of $3.87(3)\,\mu_B$ for $S = \frac{3}{2}$ with a *g* factor of 2. This indicates that Co^{2+} ions in $Co_2V_2O_7$ have a high spin state and exhibit a large orbital moment contribution in oxygen octahedral environment. Also, the negative Weiss constant with a small value shows that the interactions between Co^{2+} ions of $Co_2V_2O_7$ are of weak AF type. This is clearly different from magnetic result obtained from polycrystalline samples in Ref. [3].

To further understand the nature of magnetic ordering and anisotropy, the magnetic susceptibility and magnetization are investigated along different crystallographic *a*, *b*, and *c* axes of $Co_2V_2O_7$. As shown in Fig. 5, a clear anomaly at ~6 K in the susceptibilities is observed, confirming the occurrence of magnetic transition. We note that the susceptibility along the *b*-axis decreases more rapidly than that along another axes below ~6 K, suggesting that the *b*-axis in $Co_2V_2O_7$ is magnetic easy axis. Fig. 6 shows magnetization (*M*) as a function of applied field (*H*) at 4 K. An almost linear increase in the magnetization is observed in $H \| a$ and $H \| c$, agreeing with AF ordering below 4 K, while a rapid increase in magnetization is seen at $H = \sim 2$ T along the *b*-axis of $Co_2V_2O_7$, showing the appearance of a spin-flop-like transition. This is in good agreement with the susceptibilities in Fig. 5, supporting magnetic easy *b*-axis. However, the jump of magnetization at spin-flop-like transition is rather small, compared with expected one in simple collinear-type antiferromagnet. This suggests much complex spin structure in a skew chain with some frustration, which results in a possible partition of spin arrangements to some domains. Fig. 7 shows the result of heat capacity measurement. A sharp peak and a slight shoulder anomaly are observed at around 6.0 and 13.2 K, respectively, showing the appearance of two magnetic transitions. This indicates that a long-range magnetic ordering may start at 13.2 K and completes in a steady antiferromagnetic state at 6 K, with decreasing temperature. We note that the entropy integrated over magnetic transition at 6.0 K amounts to $\Delta S = \sim 4.785$ J/mol K, which corresponds to ~43% of $R \ln(2S+1)$ for spin $\frac{3}{2}$ systems. Such underestimation of spin entropy might be due to an overestimation of lattice contribution or a development of short-range ordering above T_N.

The combined results of magnetic and heat capacity measurements show that $Co_2V_2O_7$ is a typical 3D antiferromagnet, in which two magnetic transitions may occur at low temperature and a spin-flop-like transition may occur at the applied field along the *b*-axis. Such magnetic behaviors seem to be quite similar to those of $Ni_2V_2O_7$, which may be due to their similar crystal

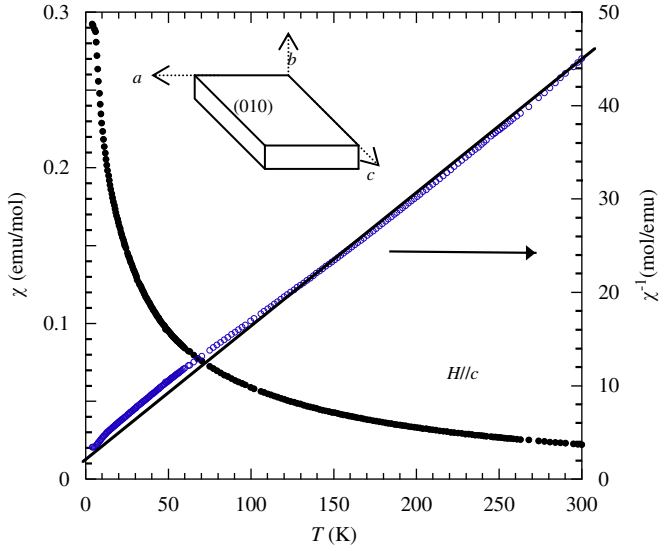

Fig. 4. Magnetic susceptibility and reciprocal one of $Ni_2V_2O_7$ measured at an applied field of 0.1 T along the *c*-axis. The image of polished sample with the crystallographic axes is seen.

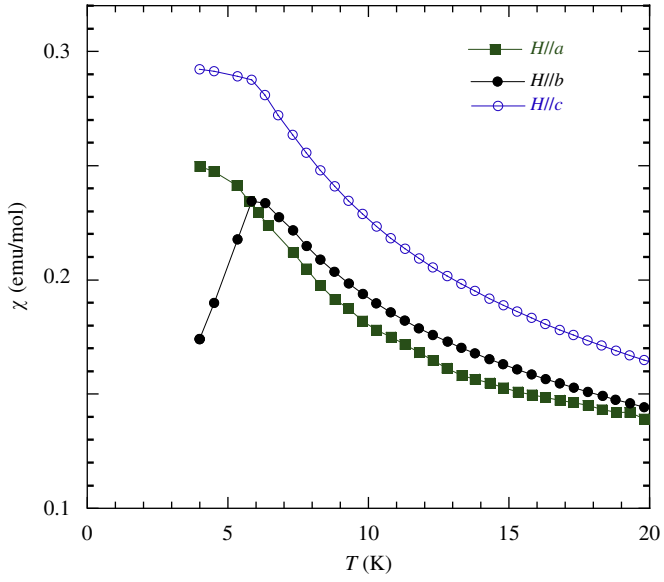

Fig. 5. An enlarged view of magnetic susceptibilities measured at low temperature along *a*-, *b*-, and *c*-axes.

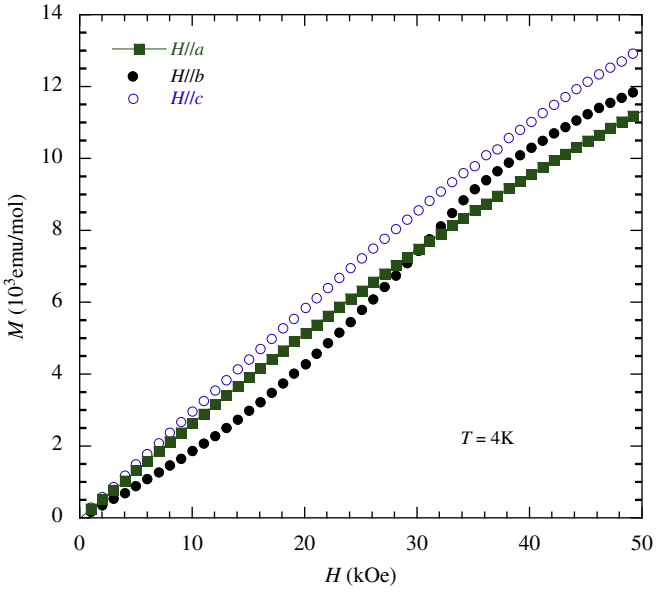

Fig. 6. Magnetization as a function of applied field at 4 K.

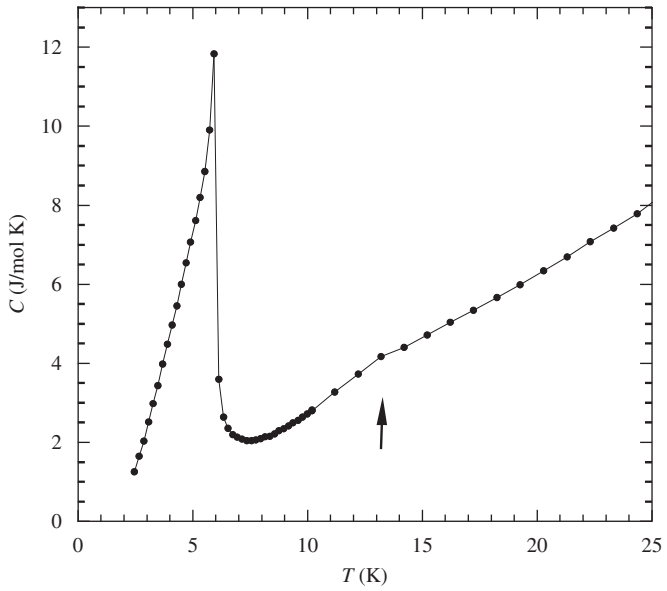

Fig. 7. Heat capacity data measured in an applied field of $H = 0$.

structure. However, magnetic transitions and magnetic easy axis are clearly different between them: $Ni_2V_2O_7$ displays three magnetic transitions and magnetic easy *a*-axis, while $Co_2V_2O_7$ displays two magnetic transitions and magnetic easy *b*-axis. We suggest that these differences may arise from magnetic natures of single-ions between Ni^{2+} and Co^{2+} ions, in which Ni^{2+} ions ($3d^8$, $t_{2g}^6e_g^2$, $S = 1$) have all t_{2g} orbits full, while Co^{2+} ions ($3d^7$, $t_{2g}^5e_g^2$, $S = \frac{3}{2}$) remain an empty t_{2g} orbit in their high spin state. Such orbital filling effects of single-ions can induce the slight different magnetic properties between nickel and cobalt oxides. A good example for this effect can also been seen in the isostructural spinel compounds $GeNi_2O_4$ and $GeCo_2O_4$ [22] or Kagome-staircase compounds $Ni_3V_2O_8$ and $Co_3V_2O_8$ [23].

4. Conclusion

We have obtained single crystals of $Co_2V_2O_7$ in a closed crucible by the flux method at a slow cooling rate. The analysis of XRD and EPMA techniques confirmed that the grown crystals have good quality. The combined results of susceptibility, magnetization, and heat capacity measurements suggested that $Co_2V_2O_7$ is a 3D antiferromagnet with two magnetic transitions at 6.0 and 13.2 K. A spin-flop-like transition was observed in the system while magnetic field was applied along the *b*-axis. By contrast to $Ni_2V_2O_7$, we suggested that similar and different magnetic properties may arise from similar crystal structure and different magnetic ions, respectively.

Acknowledgment

This work was supported in part by the National Natural Science Foundation of China under Project 20773131, the National Basic Research Program of China (No. 2007CB815307), Fujian Key Laboratory of Nanomaterials (No. 2006L2005), and Fund of Key Laboratory of Optoelectronic Materials Chemistry and Physics, Chinese Academy of Sciences (2008DP173016).

References

[1] L.A. Ponomarenko, A.N. Vasil'ev, E.V. Antipov, Y.A. Velikodny, Physica B 284–288 (2000) 1459.
[2] J. Pommer, V. Kataev, K.Y. Choi, P. Lemmens, A. Ionescu, Y. Pashkevich, A. Freimuth, G. Guntherodt, Phys. Rev. B 67 (2003) 214410.
[3] M. Touaiher, K. Rissouli, K. Benkhouja, M. Taibi, J. Aride, A. Boukhari, B. Heulin, Mater. Chem. Phys. 85 (2004) 41.
[4] A.M. Buckley, S.T. Bramwell, P. Day, D. Visser, J. Solid State Chem. 115 (1995) 229.
[5] D.C. Fowlis, C.V. Stager, Can. J. Phys. 47 (1969) 371.
[6] J.H. Liao, F. Leroux, C. Payen, D. Guyomard, Y. Piffard, J. Solid State Chem. 121 (1996) 214.
[7] J.B. Forshty, C. Wlkinson, S. Paster, B.M. Wankiyn, J. Phys.: Condens. Matter 1 (1989) 169.
[8] C. Parada, J. Perles, R. Saez-Puche, C. Ruiz-Valero, N. Snejko, Chem. Mater. 15 (2003) 3347.
[9] J. Dojcilovic, L. Novakovic, M.M. Napijalo, M.L. Napijalo, Mater. Chem. Phys. 39 (1994) 76.
[10] M. Weil, C. Lengauer, E. Füglein, E.J. Baran, Cryst. Growth Des. 4 (2004) 1229.
[11] Z. He, Y. Ueda, Phys. Rev. B 77 (2008) 052402.
[12] Z. He, Y. Ueda, J. Solid State Chem. 181 (2008) 235.
[13] Z. He, Y. Ueda, M. Itoh, Solid State Commun. 147 (2008) 138.
[14] E.E. Sauerbrei, R. Faggiani, C. Calvo, Acta Crystallogr. B 30 (1974) 2907.
[15] Z. He, J. Yamaura, Y. Ueda, W. Cheng, Phys. Rev. B 79 (2009) 092404.
[16] F. Izumi, T. Iketa, Mater. Sci. Forum 321–324 (2000) 198.
[17] E.M. Levin, C.R. Robbins, H.F. Mcmurdie, Phase Diagrams for Ceramists, American Ceramic Society, 1964 (No. 55).
[18] Z. He, J. Yamaura, Y. Ueda, W. Cheng, J. Am. Chem. Soc. 131 (2009) 7554.
[19] Z. He, T. Taniyama, M. Itoh, Y. Ueda, Cryst. Growth Des. 7 (2007) 1055.
[20] Z. He, Y. Ueda, J. Crystal Growth 310 (2008) 171.
[21] Z. He, Y. Ueda, J. Solid State Chem. 181 (2008) 2346.
[22] S. Diaz, S. de Brion, G. Chouteau, P. Canals, J.R. Carvajal, H. Rakoto, J.M. Broto, J. Appl. Phys. 97 (2005) 10A512.
[23] N. Rogado, G. Lawes, D.A. Huse, A.P. Ramirez, R.J. Cava, Solid State Commun. 124 (2002) 229.